

論文 / 著書情報
Article / Book Information

Title	Design Method for Base-isolation structure combined with Active Control Based on the Limitation Conditions of the Responses and Control Force
Authors	Yinli Chen, Daiki Sato, Kou Miyamoto, Jinhua She
Citation	Proceedings of 16th World Conference on Seismic Isolation, Energy Dissipation and Active Vibration Control of Structures, ,
Pub. date	2019, 7
URL	www.16wcsi.org
Note	This article was submitted to 16th World Conference on Seismic Isolation, Energy Dissipation and Active Vibration Control of Structures.



DESIGN METHOD FOR BASE-ISOLATION STRUCTURE COMBINED WITH ACTIVE CONTROL BASED ON THE LIMITATION CONDITIONS OF THE RESPONSES AND CONTROL FORCE

Yinli CHEN¹, Daiki SATO², Kou MIYAMOTO³ and Jinhua SHE

ABSTRACT

The linear quadratic regulator (LQR) is widely used in active structural controls (ASCs). However, at the present stage, the influence of the design parameters (LQR weighing matrices) on the vibration characteristics of the control system has not been explicitly expressed. In particular, the estimation of the required control force has not been conducted. Therefore, the LQR weighting matrices are mainly selected by trial and error approach, making it very difficult to design a control system that achieves the desired performance. To solve this problem, an equivalent model of the single-degree-of-freedom active model (structure with active control) is constructed, using which, a calculation method for the weighing matrices that does not require a trial and error approach to satisfy the desired control performance is proposed. Thereafter, the concept of the transitional response spectrum, which is widely used in structural design, is promoted as a control force spectrum that can be used to estimate the maximum control force. Finally, the design of a passive base isolation (PBI) reactor is discussed as an example, and the performance-oriented design method for the PBI structure combined with ASC is proposed that simultaneously satisfies the limitation conditions of the responses and control force.

Keywords: Active structure control; Base-isolation structure; Linear-quadratic regulator (LQR), Equivalent model

1. INTRODUCTION

To minimize damages to superstructures due to violent earthquakes and to resume operation immediately after earthquakes, in Japan, the use of passive base isolation (PBI) structures increased sharply after the great Hanshin earthquake (Y. Tanaka *et al.*, 2011). At present, the PBI structure is widely used globally, not only in public buildings and high-rise apartments, but also in major constructions (G. P. Warn *et al.*, 2012). Applying the PBI structure to nuclear power stations is a topic of worldwide research (S. Ryu *et al.*, 2013, N. Takemi *et al.*, 2013, A. S. Whittaker *et al.*, 2014, H. Asano *et al.*, 2014 and M. Kumar *et al.*, 2017). However, by the end of 2017, there were no instances of nuclear power stations using the PBI structure in Japan (T. Hiraki *et al.*, 2017). A possible reason for this is that though the PBI structure can decrease the absolute acceleration response on superstructures, it is difficult to control the displacement response within the allowable range, because the natural period of the PBI layer is relatively long (M. Kumar *et al.*, 2017). To solve this problem, the authors conducted research on the PBI structure combined with active structural control (ASC) (Y. Chen *et al.*, 2018 and K. Miyamoto *et al.*, 2018). The linear quadratic regulator (LQR) is a

¹Graduate student, Department of Architecture and Building Engineering, Tokyo Institute of Technology, Yokohama, Japan, chen.y.at@m.titech.ac.jp

²Associate professor, Laboratory for Future Interdisciplinary Research of Science and Technology (FIRST), Tokyo Institute of Technology, Yokohama, Japan, sato.d.aa@m.titech.ac.jp

³Doctor student, Department of Architecture and Building Engineering, Tokyo Institute of Technology, Yokohama, Japan, miyamoto.k.ag@m.titech.ac.jp

⁴ Professor, Department of Mechanical Engineering, Tokyo University of Technology, Hachioji, Japan, she@stf.teu.ac.jp

widely used method in ASC controller design. The controller designed by LQR ensures asymptotic stability and minimizes control energy (A. Preumont *et al.*, 2008). Thus, LQR is suitable for vibration control, and is widely used in ASCs (F. Casciati *et al.*, 2012 and S. Korkmaz *et al.*, 2011).

In conventional structural design, by using the response spectra of earthquake waves, it is possible to estimate the maximum responses of the model, without the need of numerical simulations. If the equivalent natural period and equivalent damping ratio of the ASC model can be described theoretically, the response spectrum can be used at the controller design stage, and the controller design can be simplified. However, at the present stage, using the LQR weighing matrices as parameters of LQR design, the effects on the equivalent natural period and the equivalent damping ratio of the control system are ambiguous. Hence the LQR weighing matrices are chosen using a trial and error approach, to achieve the desired control performance (A. Preumont *et al.*, 2008). To solve this problem, T. Fujii *et al.* considered the single degree of freedom (SDOF) semi-active structural control system as a research topic, and theoretically clarified the influence of the LQR weighing matrices on the vibration characteristics of the control system (T. Fujii *et al.*, 2013). However, the model used in T. Fujii *et al.* did not consider the structural internal damping, thus limiting its fields of application, making it incompatible with the model of the PBI structure combined with ASC. On the other hand, V. K. Elumalai *et al.* considered the SDOF magnetic levitation system as a research topic, and the paper proposed an algebraic method for calculating the LQR weighing matrices, which achieves the equivalent natural angular frequency and equivalent damping ratio (V. K. Elumalai *et al.*, 2017). However, V. K. Elumalai *et al.* did not investigate the impact of specific factors on control system vibration characteristics, making it difficult to use the proposed method in ASC design. Moreover, when ASC is applied in construction, the required control input can be significantly large, as expected. It is therefore necessary to deduce the theoretical equation that can be used to theoretically estimate the maximum control force.

In this paper, the performance-oriented design method is proposed that simultaneously satisfies the limitation conditions of the responses and control force. Moreover, it requires neither trial and error nor numerical simulations, which simplifies the controller design.

The equivalent model [Figure 1(b)] of the active model [Figure 1(a)], considering structural internal damping, is constructed. The influence of the design parameters (weighing matrices) on the structural characteristics (stiffness coefficient and damping coefficient) and vibration characteristics (natural period and damping ratio) is theoretically clarified. A calculation method for the LQR weighing matrices is proposed by using the constructed equivalent model to achieve the desired equivalent natural period and equivalent damping ratio. Furthermore, a new spectrum of a specific earthquake wave called the control force spectrum is proposed, which can be used to estimate the necessary maximum control force at the controller design stage. This makes it possible to calculate the weighing matrices for the design of the controller, which simultaneously satisfy the limitation conditions of responses and control force. Moreover, it requires neither trial and error nor numerical simulations. The remainder of the paper is organized as follows.

The mathematical modeling of the SDOF active model is presented in Section 2. Section 3 presents the construction of the equivalent model of the active model, considers the influence of the weighing matrices on the structural characteristics of the equivalent model, and details the calculation method for the weighing matrices. A control force spectrum is proposed in Section 4. In Section 5, a controller design method for the PBI structure with ASC that simultaneously satisfies the limitation conditions of responses and control force is proposed. Section 5 also presents a discussion of the design of the PBI type reactor as an example, to confirm the validity of the proposed design method.

2. DESIGN OF CONTROL SYSTEM

Given that it is necessary to solve the algebraic Riccati equation (ARE), the structure is assumed to be an SDOF model. The dynamics of an SDOF control system are described by the following equation:

$$m\ddot{x}(t) + c_0\dot{x}(t) + k_0x(t) = d(t) - u(t) \quad (1)$$

where m is the mass; c_0 is the damping coefficient; k_0 is the stiffness coefficient of the structure, which is defined by (2) and (3); $x(t)$, $d(t)$, and $u(t)$ are the response displacement, disturbance force, and control force, respectively.

$$k_0 = \frac{4\pi^2 \cdot m}{T_0^2} \quad (2)$$

$$c_0 = 2\zeta_0 \sqrt{m \cdot k_0} \quad (3)$$

where T_0 is the natural period of the structure, and ζ_0 is the damping ratio.

The state-space representation of (1) is

$$\dot{z}(t) = Az(t) + B_d d(t) - B_u u(t) \quad (4)$$

where $z(t)$ is a state vector, A is a system matrix, B_u is input matrices for $u(t)$, B_d is input matrices for $d(t)$, which is defined by (5).

$$z(t) = [x(t) \quad \dot{x}(t)]^T \quad (5a)$$

$$A = \begin{bmatrix} 0 & 1 \\ -\frac{k_0}{m} & -\frac{c_0}{m} \end{bmatrix} \quad (5b)$$

$$B_u = B_d = \begin{bmatrix} 0 & \frac{1}{m} \end{bmatrix}^T \quad (5c)$$

Figure 2 presents the block diagram of the control system used in this study.

The feedback control law

$$u(t) = K_P \cdot z(t) \quad (6)$$

is used, where K_P is the state-feedback gain that is designed using the LQR method, which determines the state-feedback gain by minimizing the following performance index:

$$J = \int_0^{\infty} (z(t)^T Q z(t) + u(t)^T R u(t)) dt \quad (7)$$

where $R (> 0)$ is the weighing matrix for the control force, and Q is the weighing matrix (semi-positive) defined by

$$Q = \begin{bmatrix} q_1 & 0 \\ 0 & q_2 \end{bmatrix} \quad (8)$$

Thus, K_P is defined as

$$K_P = R^{-1} B_u^T P \quad (9)$$

where P is a semi-positive symmetrical solution of the following ARE:

$$A^T P + PA - P B_u R^{-1} B_u^T P + Q = 0 \quad (10)$$

3. EQUIVALENT MODEL

3.1 Solution of the ARE

Given that the solution of the ARE is a symmetrical matrix, it is written as

$$P = \begin{bmatrix} p_{11} & p_{12} \\ p_{12} & p_{22} \end{bmatrix} \quad (11)$$

Substituting (5), (8), and (11) into (10) yields

$$\begin{bmatrix} 0 & -\frac{k_0}{m} \\ 1 & -\frac{c_0}{m} \end{bmatrix} \begin{bmatrix} p_{11} & p_{12} \\ p_{12} & p_{22} \end{bmatrix} + \begin{bmatrix} p_{11} & p_{12} \\ p_{12} & p_{22} \end{bmatrix} \begin{bmatrix} 0 & 1 \\ -\frac{k_0}{m} & -\frac{c_0}{m} \end{bmatrix} \\ - \begin{bmatrix} p_{11} & p_{12} \\ p_{12} & p_{22} \end{bmatrix} \begin{bmatrix} 0 \\ 1 \\ m \end{bmatrix} \frac{1}{R} \begin{bmatrix} 0 & 1 \\ m & p_{12} & p_{22} \end{bmatrix} \\ + \begin{bmatrix} q_1 & 0 \\ 0 & q_2 \end{bmatrix} = \begin{bmatrix} 0 & 0 \\ 0 & 0 \end{bmatrix} \quad (12)$$

Rewriting (12) yields

$$\begin{bmatrix} -2\frac{k_0}{m}p_{12} + q_1 - \frac{p_{12}^2}{m^2R} \\ p_{11} - \frac{c_0}{m}p_{12} - \frac{k_0}{m}p_{22} - \frac{p_{12}p_{22}}{m^2R} \\ p_{11} - \frac{c_0}{m}p_{12} - \frac{k_0}{m}p_{22} - \frac{p_{12}p_{22}}{m^2R} \\ 2p_{12} - 2\frac{c_0}{m} + q_2 - \frac{p_{22}^2}{m^2R} \end{bmatrix} = \begin{bmatrix} 0 & 0 \\ 0 & 0 \end{bmatrix} \quad (13)$$

Expanding (13) yields

$$-2\frac{k_0}{m}p_{12} + q_1 - \frac{p_{12}^2}{m^2R} = 0 \quad (14a)$$

$$2p_{12} - 2\frac{c_0}{m} + q_2 - \frac{p_{22}^2}{m^2R} = 0 \quad (14b)$$

$$p_{11} - \frac{c_0}{m}p_{12} - \frac{k_0}{m}p_{22} - \frac{p_{12}p_{22}}{m^2R} = 0 \quad (14c)$$

The elements of the P matrix, such as p_{11} , p_{12} , and p_{22} are obtained using the ARE in (10):

$$p_{12} = -mk_0R \pm \sqrt{m^2k_0^2R^2 + m^2q_1R} \quad (15)$$

$$p_{22} = -mc_0R \pm \sqrt{m^2c_0^2R^2 + 2m^2Rp_{12} + m^2q_2R} \quad (16)$$

$$p_{11} = \frac{c_0}{m}p_{12} + \frac{k_0}{m}p_{22} + \frac{p_{12}p_{22}}{m^2R} \quad (17)$$

Moreover, given that P is a semi-positive matrix, it yields

$$p_{11} > 0, p_{22} > 0, p_{11} \cdot p_{22} > p_{12}^2 \quad (18)$$

Finally, p_{12} and p_{22} are defined as

$$p_{12} = -mk_0R + \sqrt{m^2k_0^2R^2 + m^2q_1R} \quad (19a)$$

$$p_{22} = -mc_0R + \sqrt{m^2c_0^2R^2 + 2m^2Rp_{12} + m^2q_2R} \quad (19b)$$

From (17) and (19), the analytical solution of the ARE can be obtained using the SDOF model.

3.2 Construction of the equivalent mode

Substituting (5c) and (11) into (9), K_P is

$$\begin{aligned} K_P &= R^{-1}B_u^T P = \frac{1}{R} \begin{bmatrix} 1 & 0 \\ 0 & 1 \end{bmatrix} \begin{bmatrix} p_{11} & p_{12} \\ p_{12} & p_{22} \end{bmatrix} \\ &= \begin{bmatrix} \frac{p_{12}}{mR} & \frac{p_{22}}{mR} \end{bmatrix} = [K_{P1} \quad K_{P2}] \end{aligned} \quad (20)$$

where K_{P1} and K_{P2} are

$$K_{P1} = \sqrt{k_0^2 + q_1} \frac{1}{R} - k_0 \quad (21a)$$

$$K_{P2} = \sqrt{c_0^2 - 2mk_0 + 2\sqrt{m^2k_0^2 + m^2q_1} \frac{1}{R} + q_2} \frac{1}{R} - c_0 \quad (21b)$$

Substituting (20) and (5a) into (6) yields the control force:

$$\begin{aligned} u(t) &= K_P \cdot z(t) = [K_{P1} \quad K_{P2}] \begin{bmatrix} x(t) \\ \dot{x}(t) \end{bmatrix} \\ &= K_{P1} \cdot x(t) + K_{P2} \cdot \dot{x}(t) \end{aligned} \quad (22)$$

Substituting (22) into (1) gives the vibration equation of the equivalent model:

$$m\ddot{x}(t) + (c_0 + K_{P2})\dot{x}(t) + (k_0 + K_{P1})x(t) = d(t) \quad (23)$$

$$m\ddot{x}(t) + c_{eq}\dot{x}(t) + k_{eq}x(t) = d(t)$$

where k_{eq} and c_{eq} represent the stiffness coefficient and damping coefficient of the equivalent model and are defined by the following equation.

$$k_{eq} = k_0 + K_{P1} \quad (24a)$$

$$= \sqrt{k_0^2 + q_1 \frac{1}{R}}$$

$$c_{eq} = c_0 + K_{P2} \quad (24b)$$

$$= \sqrt{c_0^2 - 2mk_0 + 2\sqrt{m^2k_0^2 + m^2q_1 \frac{1}{R}} + q_2 \frac{1}{R}}$$

From (24a), it can be seen that k_{eq} is dependent on k_0 , q_1 , and R . When $q_1=0$, the value of k_{eq} is equal to k_0 . When q_1 is increased, the value of k_{eq} increases. When the value of R is sufficiently large, the value of k_{eq} approaches k_0 .

From (24b), it can be seen that c_{eq} is dependent on c_0 , k_0 , m , q_1 , q_2 , and R . When $q_1=q_2=0$, the value of c_{eq} is equal to c_0 . When q_1 or q_2 is increased, the value of c_{eq} increases. However, the influence of q_1 on c_{eq} is smaller than that of q_2 , given that q_1 is in the double route. When the value of R is sufficiently large, the value of c_{eq} approaches c_0 .

As is commonly known, the natural angular frequency ω_{eq} , natural period T_{eq} , and damping ratio ζ_{eq} of the equivalent model are

$$\omega_{eq} = \sqrt{\frac{k_{eq}}{m}} \quad (25a)$$

$$T_{eq} = \frac{2\pi}{\omega_{eq}} \quad (25b)$$

$$\zeta_{eq} = \frac{c_{eq}}{2m\omega_{eq}} \quad (25c)$$

In addition, the control force of the equivalent model can be obtained by the difference between (1) and (23).

$$u(t) = (k_0 - k_{eq})x(t) + (c_0 - c_{eq})\dot{x}(t) \quad ()$$

From (26), the control force of the equivalent model can be calculated using the responses of the equivalent model and k_0 , k_{eq} , c_0 and c_{eq} .

Solving (24a) and (24b), the elements of Q , such as q_1 and q_2 , can be determined by

$$q_1 = (k_{eq,tar}^2 - k_0^2)R \quad (27a)$$

$$q_2 = \left(c_{eq,tar}^2 - c_0^2 + 2mk_0 - 2\sqrt{m^2k_0^2 + m^2q_1 \frac{1}{R}} \right)R \quad (27b)$$

Furthermore, if the control system is represented in a controllable canonical form, (27) is identical to that proposed by V. K. Elumalai *et al.*

The calculation procedure of the LQR weight selection method is summarized below.

- Step 1. Specify the natural period and damping ratio of the structure (T_0 and ζ_0), and calculate the value of k_0 and c_0 using (2) and (3).
- Step 2. Specify the desired natural period and damping ratio of the control system ($T_{eq,tar}$ and $\zeta_{eq,tar}$), and calculate the value of $k_{eq,tar}$ and $c_{eq,tar}$ using (2) and (3).
- Step 3. Arbitrarily assign a value to R . Even if the value of R is arbitrary, it does not affect the control system in this design procedure.
- Step 4. Substitute $k_{eq,tar}$, k_0 , and R into (27a), and calculate q_1 in the weighing matrix Q .
- Step 5. Substitute $c_{eq,tar}$, m , k_0 , c_0 , R , and q_1 calculated in Step 4 into (27b), and calculate q_2 in the weighing matrix Q . If $q_2 \geq 0$, use the calculated values of q_1 and q_2 to design the control system. If $q_2 < 0$ because the semi-positive limitation of Q cannot be satisfied, go back to Step 2 and review $T_{eq,tar}$ or $\zeta_{eq,tar}$.

Figure 3 presents the flowchart for the calculation method of the weighing matrices.

4. CONTROL FORCE SPECTRUM

This section presents the calculation of the theoretical formula for the maximum necessary control force, and the proposal of the control force spectrum.

From (24a) and (24b), when $q_1=0$, the equivalent stiffness coefficient k_{eq} and equivalent damping coefficient c_{eq} are expressed by the following equations:

$$k_{eq} = \sqrt{k_0^2 + q_1 \frac{1}{R}} = k_0 \quad (28a)$$

$$\begin{aligned} c_{eq} &= \sqrt{c_0^2 - 2mk_0 + 2\sqrt{m^2k_0^2 + m^2q_1 \frac{1}{R}} + q_2 \frac{1}{R}} \\ &= \sqrt{c_0^2 + q_2 \frac{1}{R}} \end{aligned} \quad (28b)$$

Therefore, at $q_1=0$, the equivalent natural angular frequency ω_{eq} , the equivalent natural period T_{eq} , and the equivalent damping ratio ζ_{eq} are given by the following equations, respectively:

$$\omega_{eq} = \omega_0 \quad (29a)$$

$$T_{eq} = T_0 \quad (29b)$$

$$\zeta_{eq} = \frac{c_{eq}}{2m\omega_{eq}} = \frac{c_{eq}}{2m\omega_0} = \frac{\sqrt{c_0^2 + q_2 \frac{1}{R}}}{2m\omega_0} \quad (29c)$$

From (28), it can be seen that by setting $q_1 = 0$, the equivalent damping ratio ζ_{eq} can be adjusted without changing the equivalent natural period T_{eq} from initial natural period T_0 . By substituting (28a) into (26), the following equation can be obtained:

$$u(t) = (c_0 - c_{eq})\dot{x}(t) \quad (30)$$

Furthermore, by dividing (30) by the weight of the model m , the shear force coefficient of the control force C_u can be obtained.

$$C_u(t) = \frac{u(t)}{mg} = \frac{(c_0 - c_{eq})}{mg} \dot{x}(t) \quad (31)$$

where g is the gravitational acceleration. Therefore, the shear force coefficient of the maximum necessary control force $C_{u,peak}$ can be calculated using the following equation:

$$\begin{aligned} C_{u,peak} &= \frac{(c_0 - c_{eq})}{mg} \cdot \text{Peak}\{\dot{x}(t)\} \\ &= \frac{(c_0 - c_{eq})}{mg} \cdot S_V(T_0, \zeta_{eq}) \end{aligned} \quad (32)$$

where $S_V(T_0, \zeta_{eq})$ is the value of the response velocity spectrum when the equivalent natural period is T_0 and the equivalent damping ratio is ζ_{eq} . Moreover, by substituting $c_0=2\zeta_0\omega_0m$ and $c_{eq}=2\zeta_{eq}\omega_0m$ into (32), the shear force coefficient spectrum of the control force (control force spectrum) is

$$\begin{aligned} S_C(T_0, \zeta_0, \zeta_{eq}) &= \frac{(2\zeta_{eq}\omega_0m - 2\zeta_0\omega_0m)}{mg} \cdot S_V(T_0, \zeta_{eq}) \\ &= \frac{2\omega_0(\zeta_{eq} - \zeta_0)}{mg} \cdot S_V(T_0, \zeta_{eq}) \end{aligned} \quad (33)$$

From (33), by setting $q_1=0$, the control force spectrum S_C is calculated without using a time domain numerical simulation. By the velocity response spectrum of the earthquake wave S_V , it is possible to evaluate the magnitude of the control force. Moreover, if the initial natural period T_0 and the equivalent damping ratio ζ_{eq} are fixed, the maximum control force is proportional to the initial damping ratio ζ_0 .

5. DESIGN METHOD FOR PBI STRUCTURE WITH ASC

In this section, a controller design method for the PBI structure with ASC, which can satisfy response limitations and control force limitations simultaneously, is proposed using the weighing matrices calculation formulas (27) and the control force spectrum (33). Moreover, the design of the PBI type reactor with ASC is considered as an example, to confirm the validity of the design method.

5.1 Publication Quality and Uniformity

Step 0. Specify the following:

- mass of structure m
- earthquake used in design procedure
- limitation of response displacement x_{lim}
- limitation of response velocity \dot{x}_{lim}
- limitation of response absolute acceleration $\{\ddot{x} + \ddot{x}_g\}_{lim}$
- limitation of initial damping ratio (passive damper) $\zeta_{0,lim}$
- limitation of shear force coefficient of control force $C_{u,lim}$

- Step 1. Select the equivalent model (equivalent natural period T_{eq} and equivalent damping ratio ζ_{eq}) that satisfies the limitation conditions of the responses (displacement, velocity, and acceleration) in Step 0, From the response spectrum.
- Step 2. Using the control force spectrum (33) of the earthquake wave used in the design procedure, select the model that satisfies the limitation of the shear force coefficient of the control force $C_{u,lim}$ and the limitation of the initial damping ratio $\zeta_{0,lim}$, from the equivalent models selected in Step 1. Specify the initial damping ratio ζ_0 of the equivalent model.
- Step 3. Arbitrarily assign a value to R , set $q_1=0$, and calculate q_2 using (27b) for the selected models.
- Step 4. Calculate the state feedback gain K_P by (9), using the weighing matrices Q and R determined in Step 3.
- Step 5. Confirm if the designed controller satisfies the limitation conditions, using a time domain numerical simulation.

5.2 Required Registration

An artificial earthquake wave is used, specifically, Art Hachinohe (phase characteristic: Hachinohe 1968 EW), which has a pseudo velocity response spectrum pS_V of 200 cm/s ($\zeta=0.05$) in the region after the corner period 0.64 s (Figure 4). In addition, the disturbance force $d(t)$ is calculated by the following equation:

$$d(t) = -m\ddot{x}_g(t) \quad (34)$$

The structure is a PBI reactor building, and the mass of the structure is approximately 3.7×10^8 kg (S. Ryu *et al.*, 2013).

Step 0. Limitation conditions:

- $x_{lim} = 40$ cm
- $\dot{x}_{lim} = 150$ cm/s
- $\{\ddot{x} + \ddot{x}_g\}_{lim} = 300$ cm/s²
- $\zeta_{0,lim} = 0.1$
- $C_{u,lim} = 0.1$

- Step 1. Figure 5 presents the relationship between S_D and S_A of Art Hachinohe, and Figure 6 presents the S_V of Art Hachinohe. Given that the reduction in responses is not expected even if the equivalent attenuation factor is set to 0.4 or more, the equivalent attenuation factor was examined up to 0.4. Table 1 presents the six models satisfying the response limitation conditions of Step 0.
- Step 2. Using (33), Figure 7 presents the relationship between the initial damping ratios ζ_0 and peak shear force coefficient of control force $C_{u,peak}$ of the six models selected in Step 1 and the maximum shear force coefficients of the control force $C_{u,peak}$. From Figure 7, only the model with the equivalent natural period $T_{eq}=2.5$ s and equivalent damping ratio $\zeta_{eq}=0.2$ satisfies the limitation condition of the initial damping ratio of $\zeta_{0,lim}$ and shear force coefficient of the control force $C_{u,lim}$.

Moreover, the model with the initial damping ratio $\zeta_0=0.05$ has a relatively less passive damper, and is therefore a passive-damper sensitive model (Model 1). The model with the initial damping ratio of $\zeta_0=0.1$ has a relatively low control force, and is therefore a control-force sensitive model (Model 2). In addition, to realize the equivalent model with the equivalent damping ratios of 0.3 and 0.4, it is necessary to increase $C_{u,lim}$ or $\zeta_{0,lim}$.

Step 3. Fixing $R=1$ and $q_1=0$, calculate q_2 using (27b). Table 2 presents q_2 calculated using (27b).

Step 4. Table 3 presents the state feedback gain K_P of Models 1 and 2, calculated using (21).

Step 5. Figure 8 presents the responses (displacement x , velocity \dot{x}_{lim} , and absolute acceleration $\{\ddot{x} + \ddot{x}_g\}_{lim}$) and the shear force coefficient of the control force C_u of Models 1 and 2.

From the design example, the following results were obtained:

- (1) From Figures 8(a)-(c), it can be seen that Models 1 and 2 satisfy all the limitation conditions of Step 0. The validity of the proposed design method can therefore be confirmed.
- (2) From Figures 8(a)-(c), it can be seen that the responses of Models 1 and 2 are identical. It can therefore be confirmed that the equivalent natural period T_{eq} and equivalent damping ratio ζ_{eq} are the same for Models 1 and 2.
- (3) From Figure 8(d), it can be seen that the maximum shear force coefficient of the control force of Model 1 is larger than that of Model 2. This is because the initial damping ratio of Model 1 ($\zeta_0=0.05$) is smaller than that of Model 2 ($\zeta_0=0.10$).

6. CONCLUSIONS

In this study, an equivalent model of an active model with a controller designed using an LQR was constructed for an SDOF model. This paper also presents the calculation method for determining the weighing matrices to satisfy the desired equivalent natural period T_{eq} and equivalent damping ratio ζ_{eq} , using the constructed equivalent model. Furthermore, in this paper, the control force spectrum is proposed, which can be used estimate the maximum necessary control force. This makes it possible to design a controller that satisfies the limitation conditions of the responses and maximum control force without trial and error, by using the conventional response spectrum of an earthquake. In the numerical design example of the PBI type reactor building with ASC, the validity of the proposed design method is verified. This study clarified the following points:

- (1) The analytic solution of the ARE used in the LQR can be obtained for SDOF model with damping coefficient, and the influence of the weighing matrices on vibration characteristics can be theoretically demonstrated.
- (2) By constructing an equivalent model, which has the same natural period and damping ratio as the active model, it is possible to evaluate the peak responses of the active model without the need of numerical simulations, by using the response spectrum of an earthquake wave. It is therefore possible to calculate the weighing matrices that satisfy the desired responses.

In this paper, a control force spectrum that can be used to estimate the required maximum control force for a specific earthquake wave was proposed. By using the proposed control force spectrum, the required maximum control power can be estimated at the controller design stage, without the need of numerical simulations.

7. REFERENCES

- Yuji T., Nobuo F., Jun T. and Masafumi M., (2011) Development and analysis of database for base-isolated buildings in japan. *AIJ Journal of Technology and Design*, (17): 79-84 [in Japanese].
- Warn G. P. and Ryan K. L., (2018) A Review of Seismic Isolation for Buildings: Historical Development and Research Needs. *Soil Dynamics and Earthquake Engineering*.
- Shimamoto R., Umeki Y. and Umeki Y., (2013) A study on seismic behavior of isolated reactor building in large input region. Part 1: Overall outline. *Summaries of technical papers of annual meeting, Architectural Institute of Japan*: 1285-1286 [in Japanese].

Takafumi H., Kenji K. and Haruyuki K., (2017) Mechanical energy evaluation method for seismic isolation systems with rubber bearings under large deflection. *AIJ Journal of Structural and Construction Engineering*, (82): 75-85 [in Japanese].

Vinodh K. E. and Raaja G. S., (2017) A new algebraic LQR weight selection algorithm for tracking control of 2 {DoF} torsion system. *Archives of Electrical Engineering*, (66): 55-75 [in Japanese].

Yinli C., Daiki S., Kou M. and Jinhua S., (2018) Mechanical energy evaluation method for seismic isolation systems with rubber bearings under large deflection. *AIJ Journal of Structural Engineering*, (64B): 199-206 [in Japanese].

Andre P. and Kazuto S., (2008) Active control of structures. *John Wiley & Sons, Inc.*

Fabio C., Jose R. and Umut Y., (2018) Active and semi-active control of structures – theory and applications: A review of recent advances. *Journal of Intelligent Material Systems and Structures*, (23): 1181-1195.

A. S. Whittaker, M. Kumar and M. Kumar. (2014). Seismic Isolation of Nuclear Power Plants, *Nuclear Engineering and Technology*, 46 (5), 569 – 580.

H. Asano, T. Hirotsu, T. Nakayama, T. Norimono, Y. Aikawa, K. Sato, S. Asakura, M. Jimbo and Y. Umeki. (2014). Development of an Evaluation Method for Seismic Isolation Systems of Nuclear Power Facilities: Part 10 — Evaluation of Seismic Isolator Design, in: *Proceedings of ASME 2014 Pressure Vessels & Piping Conference*, Vol. 8, California, USA, p. V008T08A017.

K. Miyamoto, D. Sato and J. She. (2018). A New Performance Index of LQR for Combination of Passive Base Isolation and Active Structural Control, *Engineering Structures*, 157, 280 – 299.

A. Preumont and A. Seto. (2008). *Active Control of Structures*, John Wiley & Sons, Inc.

F. Casciati, J. Rodellar and U. Yildirim. (2012). Active and Semi-Active Control of Structures – Theory and Applications: A Review of Recent Advances, *Journal of Intelligent Material Systems and Structures*, 23 (11), 1181–1195.

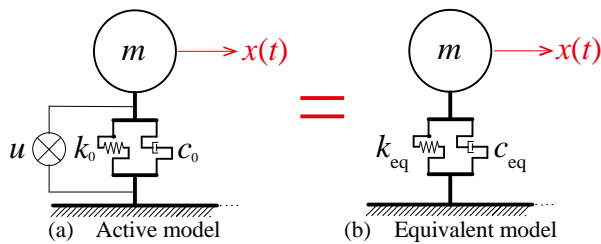


Figure 1 SDOF model with active control

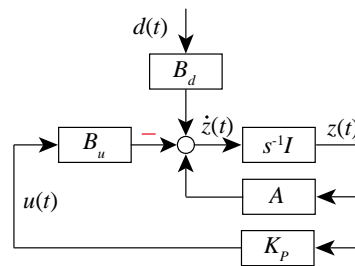


Figure 2 Block diagram of control system

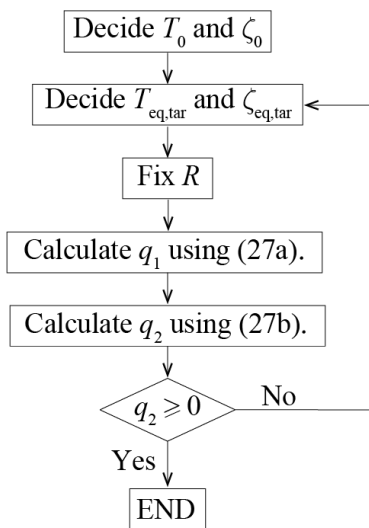
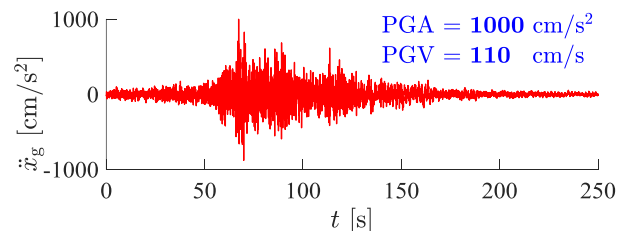
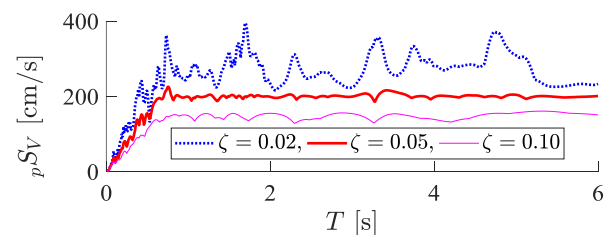


Figure 3 Flowchart of calculate procedure



(a) Accelerogram



(b) Pseudo velocity response spectrum

Figure 4 Art Hachinohe wave

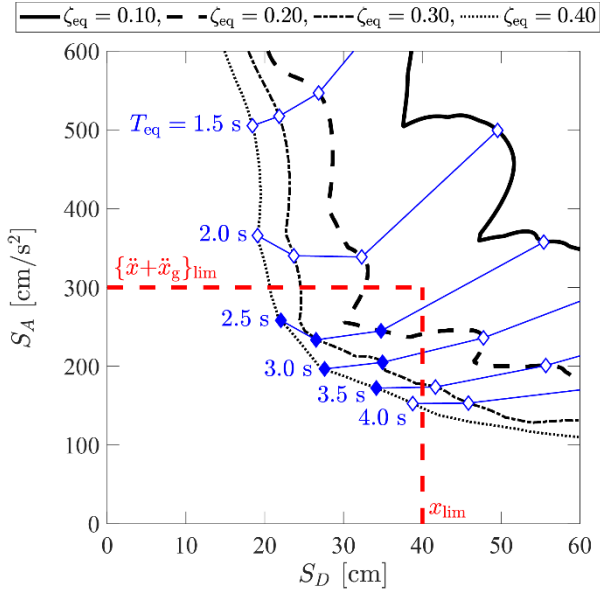


Figure 5 Relationship between S_D and S_A

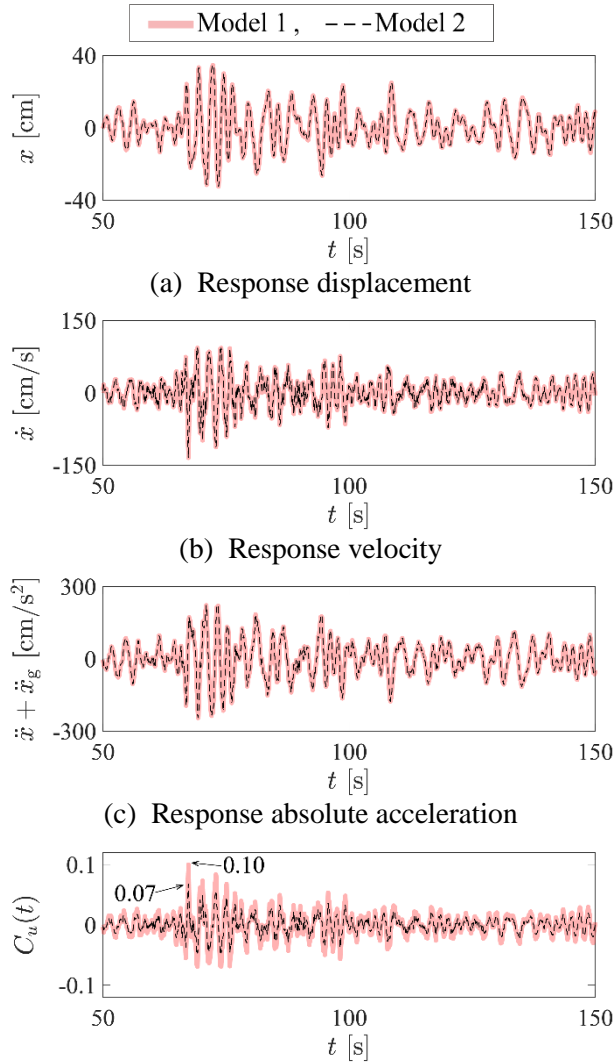


Figure 8 Numerical simulation results of models

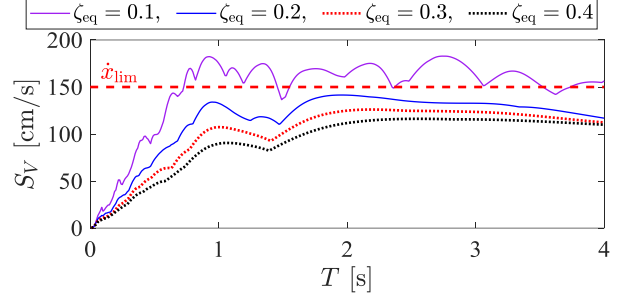


Figure 6 Velocity response spectrum

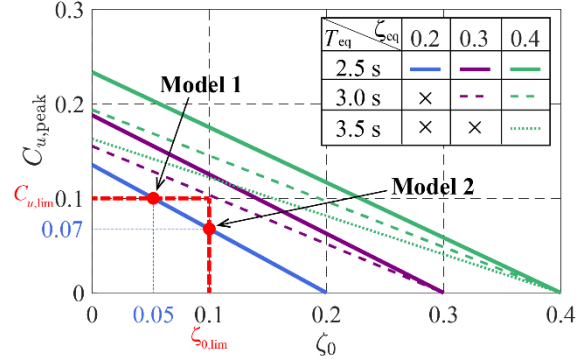


Figure 7 Relationship between ζ_0 and C_u

Table 1 Peak responses of selectable

T_{eq} [s]	2.5			3		3.5
ζ_{eq} [-]	0.2	0.3	0.4	0.3	0.4	0.4
Dis. [cm]	35	27	22	35	28	34
Vel. [cm/s]	135	125	116	124	116	113
Acc. [cm/s ²]	245	233	258	204	197	172

Table 2 Parameters of models

Name	Model 1	Model 2
m [kg]	3.7×10^8	
T_{eq} [s]	2.5	
ζ_{eq} [-]	0.20	
T_0 [s]	2.5	
ζ_0 [-]	0.05	0.10
R [-]	1	
q_1 [-]	0	
q_2 [-]	1.3×10^{17}	1.0×10^{17}

Table 3 Parameters of models

Name	Model 1	Model 2
K_{P1}	0	
K_{P2}	2.7×10^8	1.9×10^8